Engineering Biosensors with Dual Programmable Dynamic Ranges
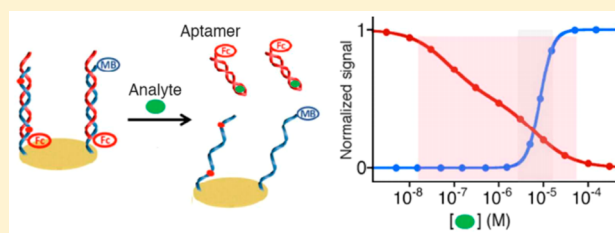
Benmei Wei,[†] Juntao Zhang,[†] Xiaowen Ou,[†] Xiaoding Lou,[†] Fan Xia,*[,†] and Alexis Vallée-Bélisle*[,‡]

[†]School of Chemistry and Chemical Engineering, Huazhong University of Science and Technology, Wuhan 430074, P. R. China
[‡]Laboratory Biosensors & Nanomachines, Département de Chimie, Université de Montréal, Montréal, Québec H3T 1J4, Canada

S *Supporting Information*

ABSTRACT: Although extensively used in all fields of chemistry, molecular recognition still suffers from a significant limitation: host−guest binding displays a fixed, hyperbolic dose−response curve, which limits its usefulness in many applications. Here we take advantage of the high programmability of DNA chemistry and propose a universal strategy to engineer biorecognition-based sensors with dual programmable dynamic ranges. Using DNA aptamers as our model recognition element and electrochemistry as our readout signal, we first designed a dual signaling "signal-on" and "signal-off" adenosine triphosphate (ATP) sensor composed of a ferrocene-labeled ATP aptamer in complex to a complementary, electrode-bound, methylene-blue labeled DNA. Using this simple "dimeric" sensor, we show that we can easily (1) tune the dynamic range of this dual-signaling sensor through base mutations on the electrode-bound DNA, (2) extend the dynamic range of this sensor by 2 orders of magnitude by using a combination of electrode-bound strands with varying affinity for the aptamers, (3) create an ultrasensitive dual signaling sensor by employing a sequestration strategy in which a nonsignaling, high affinity "depletant" DNA aptamer is added to the sensor surface, and (4) engineer a sensor that simultaneously provides extended and ultrasensitive readouts. These strategies, applicable to a wide range of biosensors and chemical systems, should broaden the application of molecular recognition in various fields of chemistry.

Biomolecular recognition, which plays a central role in biochemical processes of living organisms, also plays a key role in all fields of chemistry.[1] For the last 40 years, for example, researchers have taken advantage of the high affinity and high specificity of antibodies for their target and have used them as recognition elements of choice in various biosensing technologies.[2] In the last 10 years, DNA and RNA aptamers have also emerged as recognition elements of choice in many chemical systems.[1a,3−5] Indeed, with their small size, high stability, easiness of synthesis, and high designability, aptamers have shown significant advantages over their more complex and expensive protein counterparts. Over the last 5 years, for example, companies such as SomaLogic have developed and characterized thousands of aptamers that specifically bind to biomolecules that are diagnostic of numerous diseases.[6] Some of these aptamers have already been adapted into specific and selective sensors that perform in a variety of complex media such as whole blood.[7]

Despite their excellent performance, biosensors based on molecular-recognition still suffer from a potentially significant limitation: their single-site binding produces a fixed, hyperbolic dose−response curve which limits their useful dynamic range to a fixed 81-fold target concentration variation where the receptor occupancy, and thus the sensor signal, varies from 10% to 90%.[8] The practicability of sensors would drastically improve, for example, if their dynamic range could be optimized for any specific application. Broadening the dynamic range of biosensors would, for example, greatly improve the ability to monitor viral load[9] as well as the efficiency of biofuel cells.[10]

Narrowing the dynamic range of molecular logic gates[11] and biosensors used for therapeutic drug monitoring, would reduce noise and improve precision.[12]

Recently, we and others have proposed various strategies to tune, extend, and narrow the dynamic range of DNA-based sensors that use either optical[13] or electrochemical readouts.[14] These strategies enable one to tune the affinity of biosensors that detect nucleic acids,[15] small molecules,[16] heavy metal ions,[17] pH,[18] and temperature.[19] In addition, environmental changes and material sizes are also used to adjust the dynamic range of DNA-based sensors.[20] However, an inherent trade-off remains when utilizing those strategies: biosensors with extended dynamic range display reduced precision, while highly precise sensors display narrowed dynamic range. To circumvent these limitations, we report here the development of a novel dual-signaling biosensor architecture that simultaneously provides both a highly sensitive "signal-on" readout over a small fixed dynamic range as well as a "signal-off" readout, enabling quantification over a large, extended dynamic range.[21]

As a test bed platform for validating our strategy, we selected the well-characterized adenosine triphosphate [ATP] binding aptamer[22] and adapted it in a dual "signal-on" and "signal-off" electrochemical sensor.[21a,b] This adenosine triphosphate aptamer displays a high level of selectivity enabling one to distinguish ATP from a mixture of other analogues (e.g., CTP,
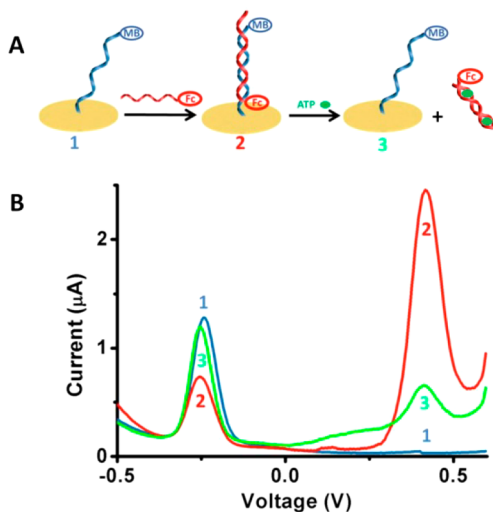
GTP, and UTP).[22b] We also selected electrochemistry as our read-out mechanism since aptamer-based electrochemical sensors have been found specific and selective enough to perform in a variety of complex media, including foodstuffs, undiluted serum, saliva, whole blood, and in the circulating blood of living animals.[3,23,24] In order to build our electrochemical dual signaling sensor, we employed a popular duplex aptamer architecture,[25] which possesses the following advantages. First, its design and thermodynamic optimization are straightforward (design of a complementary strand of optimal size). Second, its structure-switching and signaling mechanisms are universal: the DNA shifts from a duplex to a single strand conformation. Finally, although duplex aptamer sensors display response time that are slower than their unimolecular counterparts, novel selection strategies are now employed to design duplex aptamers that efficiently dissociate from their complementary DNA sequence upon target binding.[26,27] Nutiu and Li, for example, have shown that their duplex ATP sensor responds in less than 5 min in the presence of ATP.[25]

We built our dual signaling duplex sensor by employing a ferrocene[Fc]-labeled ATP binding DNA aptamer and a complementary 27-nucleotide long methylene blue[MB]-labeled capturing strand [cDNA]. We first attached a thiolated, MB-modified cDNA strand onto a gold electrode via a gold−thiol bond (Figure 1A, left). This unstructured DNA

Figure 1. (A) Schematic representation of a dual-signaling, electrochemical ATP aptamer-based sensor. This sensor consists in an ATP aptamer-cDNA duplex attached on a gold electrode that can dissociate efficiently in the presence of ATP molecules via a structure-switching mechanism.[30] (B) Square wave voltametry curves obtained for the different steps involved in the sensor preparation and use. We observe a single oxidation peak at about −0.25 V when MB-labeled cDNA is first anchored to a gold electrode (blue, line 1). After addition of the Fc-labeled DNA aptamer, we observe a diminution in the MB peak current combined to an increase in Fc oxidation peak at about 0.40 V (red, line 2). In the presence of ATP molecules, the specific ATP−aptamer interactions trigger the dissociation of the duplex sensor leading to a large increase of MB peak current and a significantly decrease of Fc peak current (green, line 3).

strand can be detected via the oxidation/reduction peak of MB at about −0.25 V (Figure 1B, blue line). After hybridization with the ferrocene [Fc]-labeled ATP DNA aptamer (Figure 1A, middle), we observe a reduction of the MB peak current consistent with the expected reduction of the collision efficiency

taking place between MB and the interrogating electrode due to a larger distance associated with the double strand DNA[24] (Figure 1B, red line). At the same time, the hybridization of the ferrocene [Fc]-labeled ATP DNA aptamer on the gold surface is also confirmed by the apparition of a new peak at 0.40 V, which is the expected potential for the ferrocene oxidation peak.[28] The presence of ATP molecules, which binds to the ATP-binding aptamer, triggers aptamer dissociation from the anchoring cDNA (Figure 1A, right) resulting in a significant reduction of Fc peak current combined with an increase in the MB peak current (Figure 1B, green line). Among others, such dual-signaling biosensors were proposed to offer various advantages for applications ranging from pathogen diagnosis,[29] to identification of target mismatch location,[30] and molecular logic gates.[31] On the other hand, the potential of such dual-signaling sensors remains relatively limited due to their fixed 81-fold dynamic range (as seen in Figure 2A).
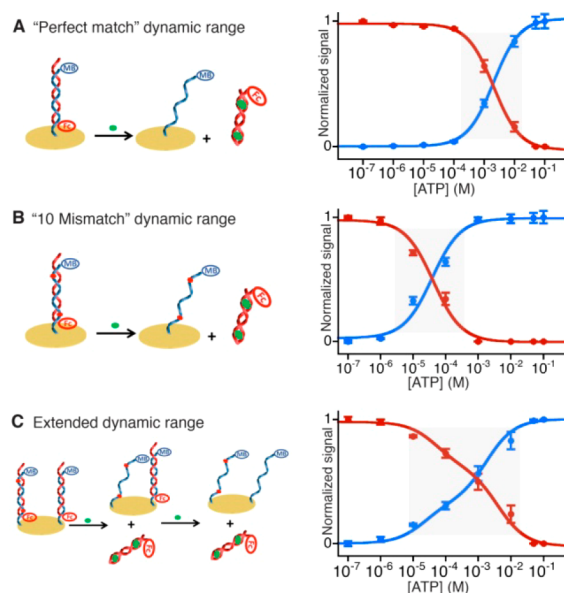

Figure 2. Schematic representation and dose−response curves of the dual signaling ATP sensor using a (A) perfect match complementary surface-bound cDNA (Sensor 1); (B) 10 mismatches complementary surface-bound cDNA (Sensor 3); and (C) using both the perfect and 10 mismatches complementary surface-bound DNA. (A) The ATP sensor with the surface-attached MB-labeled cDNA with perfect complementarity to the aptamer sequence exhibits a dissociation constant K_d of about 2.1 mM with an expected 75 to 89-fold dynamic range. (B) By introducing 10 mismatches in the cDNA (see Sensor 3, Figure S1), we can reduce the cDNA-aptamer hybridization energy and quantify 50-fold lower ATP concentrations over a dynamic range of 81-fold (K_d = 38 μM) for both the "signal-on" and "signal-off" readouts. (C) We can extend the dynamic range of the dual-signaling sensor by coimmobilizing a low-affinity dual-signaling sensor (perfect match cDNA, Sensor 1) and a higher affinity dual-signaling sensor (Sensor 3 with 10 mismatches in the cDNA) in a 1:1 ratio on a single gold electrode. The useful dynamic range of this dual-signaling sensor is now between 6000- to 7500-fold for "signal-on" and "signal-off", respectively. Data points are expressed as mean signal from three electrodes ± standard deviation.

We first tested our ability to tune the dynamic range of this dual labeled aptamer-based sensor via mutation by simply changing the level of complementarity between the aptamer and the anchoring cDNA. This can be readily achieved by introducing mismatched nucleotides in the anchoring cDNA.

Those mismatches reduce the affinity between the cDNA and the aptamer and facilitate the release of the aptamer at lower ATP concentration.[16a] In principle, this strategy should enable to increase the dissociation constant (K_d) between the sensor and the target, without affecting the specificity of the sensor since the integrity of the target binding site on the aptamer remains untouched.[16a,32] We initially performed a dose−response experiment of our "perfect match" sensor (also referred to as Sensor 1) by employing a MB-labeled 27-nucleotides cDNA that is perfectly complementary to the Fc-labeled aptamer (Figure 2A, left). This dual-signaling sensor exhibits a dissociation constant of 2.1 mM (for both "signal-on" and "signal-off" output), and its dynamic range spans the conventional 75-fold ("signal-on") and 89-fold ("signal-off") change in target concentration (i.e., target concentration variation where the sensor signal varies from 10% to 90%) (Figure 2A). We then investigated the dynamic range of dual-signaling sensors containing either 7 or 10 mismatched nucleotides in their cDNA sequences (Figure S1). At least 7 mismatches (over the 27 interacting nucleotides) are required in order to improve the affinity of the sensor (see Sensor 2 with a dissociation constant of 1.1 mM, Figure S1). In an attempt to further improve the sensor affinity for ATP, we added three additional mismatches in the cDNA (Figure 2B, left, Sensor 3). Sensor 3, with now 10 mismatched base pairs, displays a dissociation constant of 38 μM with a 81-fold dynamic range for both the "signal-off" and "signal-on" outputs (Figure 2B, right).

In order to extend the useful dynamic range of our dual-signaling sensor, we then coimmobilized on a single gold electrode with two dual-signaling sensors that differ in target affinity. To obtain the ideal trade-off between large dynamic range without compromising too much on the linearity of the output signal versus the target concentration, it was found that sensor affinities should differ by around ∼80-fold.[13,14] We thus combined an equimolar concentration of the low-affinity Sensor 1 (K_d = 2.1 mM) with the higher affinity Sensor 3 (K_d = 38 μM) (Figure 2C, left). As expected, this new heterogeneous sensor extended its dynamic range to 6000-fold ("signal-on") and 7500-fold ("signal-off") with target concentrations ranging between 8 μM and 10240 μM for the "signal-on" curve (Figure 2C, right; Figure S2).

In order to enhance the sensitivity of the dual-signaling sensor and improve its ability to measure small changes in target concentrations, we then investigated the impact of a sequestration mechanism.[33] In this mechanism, a high-affinity nonsignaling sensor is used to sequester ATP and compete for ATP binding with a low-affinity signaling sensor.[34,35] To achieve this goal, we coimmobilized on the gold surface both the unlabeled (no MB and no Fc) high-affinity Sensor 3 complex (containing 10 mismatched nucleotides) and the MB-, Fc-labeled low-affinity Sensor 1 complex ("perfect match") (Figure 3A, top). When using a 10:1 ratio of "Sensor 3/Sensor 1", the large concentration of high-affinity unlabeled Sensor 3 sequesters most of the ATP molecules as the ATP concentration remains below 3 mM (for a 5 μL volume) (Figure 3A). The high-affinity unlabeled Sensor 3 therefore acts as a depletant and sequesters the target until the ATP molecules surpasses the binding capacity of the surface-attached Sensor 3 (each aptamer is expected to bind 2 ATP molecules).[35] The threshold concentration (3 mM) therefore depends upon the depletant/sensor ratio and the sample volume (see Supporting Methods). As ATP concentration is raised above 3 mM and the depletant becomes saturated, the low-ffinity Sensor 1 becomes then saturated with
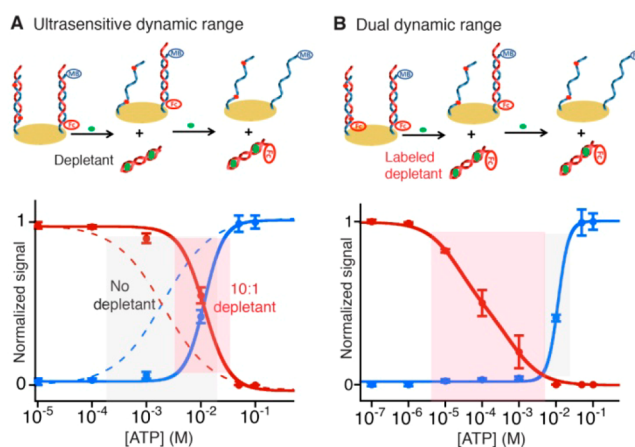

Figure 3. (A) We can narrow the dynamic range of dual-signaling electrochemical aptamer-based sensors by engineering a sequestration strategy. This can be realized by adding a nonsignaling high-affinity sensor that acts as a depletant on the sensor surface. This high-affinity depletant sequesters the target until a threshold concentration is surpassed.[31] Above this concentration, the low-affinity signaling sensor will bind any free target molecule, thus generating highly cooperative binding curves. The useful dynamic range of this sensor can then be arbitrarily narrowed down to about 6- to 10-fold by employing a 10:1 ratio of "high-affinity depletant/low-affinity sensor".[13,14] This increase in the steepness of the dose−response curve improves the ability of this sensor to detect small changes in target concentration. (B) We can engineer dual-signaling biosensors with two distinct programmable dynamic ranges by coassembling on the same surface an unlabeled high-affinity cDNA and a MB-labeled low-affinity cDNA. Both cDNAs can hybridize with the Fc-labeled ATP aptamer. When the ratio of the concentration "high-affinity to low-affinity" is near or above 1:1 (here 10:1), the dynamic range created spans 2585-fold for the "signal-off" sensor and 5-fold for the "signal-on" sensor (see Table S3 and Figure S3 for all data). Data points are expressed as mean signal from three electrodes ± standard deviation.

ATP and the sensor response curve displays a much more cooperative profile (Figure 3A, bottom). Using this strategy, we narrowed the useful dynamic range of our dual-signaling sensor down to approximately 6-fold ("signal-on") and 10-fold ("signal-off"), which enhanced the sensitivity of our sensor by up to 10-fold and improve its ability to detect small changes in target concentration near a specific target range. We also investigated the influence of the ratio of "high-affinity depletant/low-affinity sensor" on the level of cooperativity displayed by the dual-signaling sensor.[36] As predicted, we found that the steepness of the dose−response curve, and therefore the sensitivity of the sensor, increases as this ratio is increased (Tables S2 and S3). As noted previously the sequestration strategy is not without a limitation: the generation of an ultrasensitive response is achieved at the cost of a reduced affinity, which shifts the minimum target concentration producing a detectable signal (the detection limit) toward higher concentrations.[35]

The above results demonstrate strategies to tune the useful dynamic range of dual-signaling sensors so that they become either precise over a narrowed range (Figure 3A) or less precise, but still linear, over an extended dynamic range (Figure 2C). However, in all these strategies, the dynamic range is synchronously extended or narrowed for both signal outputs. In order to broaden the use of biosensors in clinical diagnostics, we thus attempted to program our dual-signaling sensor so that it produces two distinct dynamic ranges for the "signal-on" and "signal-off", respectively (Figure 3B). To do so, we first created

a highly sensitive "signal-on" sensor by employing a sequestration strategy similar to that presented in Figure 3A. To achieve this, we immobilized a 10:1 ratio of Fc single labeled Sensor 3 over Fc-, MB-labeled low-affinity Sensor 1 on an electrode. Below the threshold concentration of 3 mM, the MB signal remains minimal (this threshold depends upon the depletant/sensor ratio, the target concentration and the sample volume),[13,14] since the high-affinity Sensor 3 acts once again as a depletant and sequesters the ATP.[34] Passed the 3 mM threshold, an increase in target concentration leads to the saturation of the low-affinity Sensor 1, therefore generating a highly cooperative and precised "signal-on" MB response with 80% of the signal being generated between 5 to 23 mM ATP (5-fold dynamic range) (Figure 3B, bottom, blue curve). Alternatively, we can simultaneously create a "signal-off" output with a highly extended dynamic range going from 2 μM to 5 mM ATP with a 2585-fold dynamic range (Figure 3B, bottom, red curve).

One advantage of this dual signaling sensor is that its ultrasensitive "signal-on" readout can also be tuned to achieve optimal performance at a specific dynamic range. For example, to create a dual-signaling ATP sensor that displays optimal sensitivity at biologically relevant ATP concentrations (0.7−9 mM),[35] we simply reduced the relative amount of the high-affinity Sensor 3 depletant to 1:1. Under this condition, the dynamic range of the more cooperative "signal-on" output shifted to the biologically relevant range (0.3−16 mM) whereas the extended "signal-off" dynamic range remained nearly optimal with a 5400-fold span (Figures S3 and S4). By employing this highly tunable strategy, we can therefore engineer sensors that possess both sensitive and extended dynamic ranges simultaneously. A great advantage of this strategy is also its steadyness. In contrast to unimolecular electrochemical aptamer-based sensors, which display different gains and sensitivities to variation of probe density on the surface of the sensor,[37] the gain and tunability of dual labeled duplex aptasensors should remain relatively insensitive to probe density variation due to the universality of its structure-switching mechanisms. However, the adjustability of the dynamic ranges is limited for low concentrations ATP, which may be caused by the binding constant of aptamer itself.

In conclusion, here we have demonstrated various simple strategies to create electrochemical dual-signaling aptamer-based sensors that provide simultaneous extended and narrowed useful dynamic ranges. The approach is simple and could readily be applied on the thousand different aptamers that have been reported to date[3−6] in order to build one-step electrochemical sensors selective enough to perform in a variety of complex media.[7] More specifically, using the ATP aptamer as a model system,[21e] we first showed that we could both tune (50-fold variation), extend (up to 7500-fold) or narrowed (down to 6-fold) the useful dynamic range of a dual-signaling biosensor (Figure 4A−C). In order to improve the performance of the sensors, we also demonstrate how those dual-signaling sensors can be engineer to simultaneously provide both an extended-dynamic range ("signal-off", 2585-fold) and a narrowed, ultrasensitive dynamic-range ("signal-on", 5-fold) (Figure 4D). Such sensors could be of great interest, for example, in therapeutic drug monitoring where sensors need to be highly precise in a narrow therapeutic range but also display an extended dynamic range to enable precise drug measurements for patients that would fall out of the therapeutic range due to different pharmacokinetic.[38] The ability to create biorecognition-based sensors that provide simultaneous extended and narrowed dynamic range
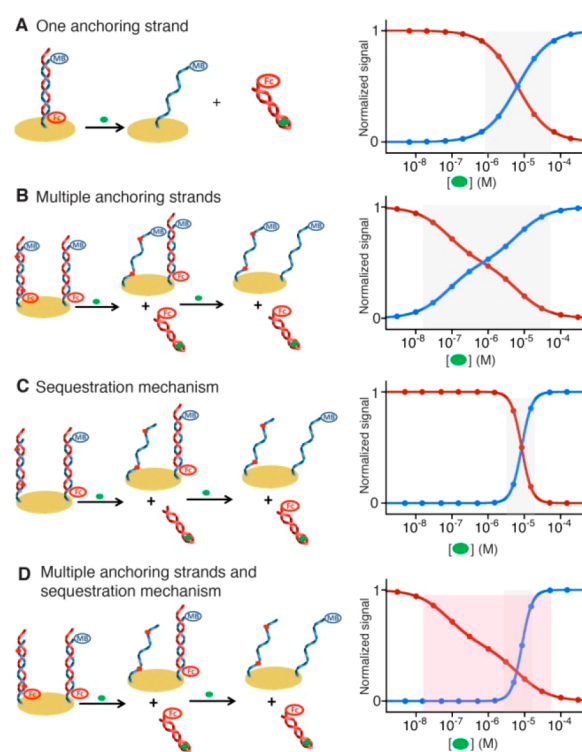

Figure 4. Universal strategies to engineer electrochemical aptamer-based sensors with dual programmable dynamic ranges. (A) A "dimeric" sensor that simultaneously provides "signal-on" and "signal-off" readout using a ferrocene-labeled DNA aptamer and a complementary anchoring DNA strand (cDNA) containing a different redox label (methylene blue). (B) Extending the dynamic range of this sensor by 2 orders of magnitude by employing two anchoring cDNAs (blue strands) displaying 81-fold difference in affinity. (C) Ultrasensitive sensor employing a sequestration mechanism via the presence of a high-affinity, nonsignaling (no redox moiety) "depletant" receptor. (D) A sensor that provides simultaneous "signal-on" extended and "signal-off" ultrasensitive dynamic responses.

also solves to an important limitation of classic bimolecular recognition systems such as biofuel cells,[10] bioelectronic "logic gates",[39] and may find applications in the many fields of chemistry that employ molecular recognition.

ASSOCIATED CONTENT

Supporting Information

The Supporting Information is available free of charge on the ACS Publications website at DOI: 10.1021/acs.analchem.7b04852.

> Experiments details of materials, the fabrication of sensors, stability and affinity of cDNA−aptamer complex, extended dynamic range of dual-signaling sensor, influences of the ratio [depletant]/[sensor] on the sensitivity of the sensor (sequestration strategy) and dynamic range of the sensor (sequestration strategy), influence of concentration ratio of high-affinity probe to low-affinity probe on gap of dynamic range, and dual-signaling ATP sensor optimized for the detection of ATP within the biologically relevant ATP range (0.7−9 mM) (PDF)

AUTHOR INFORMATION

Corresponding Authors
*E-mail: xiafan@hust.edu.cn.
*E-mail: a.vallee-belisle@umontreal.ca.

ORCID ⊙

Benmei Wei: 0000-0002-7672-1707
Fan Xia: 0000-0001-7705-4638
Alexis Vallée-Bélisle: 0000-0002-5009-7715

Notes

The authors declare no competing financial interest.

■ **REFERENCES**

(1) (a) Jhaveri, S. D.; Kirby, R.; Conrad, R.; Maglott, E. J.; Bowser, M. R.; Kennedy, T.; Glick, G.; Ellington, A. D. *J. Am. Chem. Soc.* **2000**, *122*, 2469. (b) Lehn, J. M. *Angew. Chem., Int. Ed. Engl.* **1990**, *29*, 1304. (c) Kaifer, A. E. *Acc. Chem. Res.* **1999**, *32*, 62. (d) Eliseev, A. V.; Nelen, M. I. *J. Am. Chem. Soc.* **1997**, *119*, 1147. (e) Babine, R. E.; Bender, S. L. *Chem. Rev.* **1997**, *97*, 1359.

(2) North, J. R. *Trends Biotechnol.* **1985**, *3*, 180.

(3) Cho, E. J.; Lee, J.; Ellington, A. D. *Annu. Rev. Anal. Chem.* **2009**, *2*, 241.

(4) Lollo, B.; Steele, F.; Gold, L. *Proteomics* **2014**, *14*, 638.

(5) Fang, X.; Tan, W. *Acc. Chem. Res.* **2010**, *43*, 48.

(6) Mehan, M. R.; Ayers, D.; Thirstrup, D.; Xiong, W.; Ostroff, R. M.; Brody, E. N.; Walker, J. J.; Gold, L.; Jarvis, T. C.; Janjic, N.; Baird, G. S.; Wilcox, S. K. *PLoS One* **2012**, *7*, e35157.

(7) Schoukroun-Barnes, L. R.; Macazo, F. C.; Gutierrez, B.; Lottermoser, J.; Liu, J.; White, R. J. *Annu. Rev. Anal. Chem.* **2016**, *9*, 163.

(8) (a) Koshland, D. E., Jr.; Goldbeter, A.; Stock, J. B. *Science* **1982**, *217*, 220. (b) Ferrell, J. E., Jr. *Trends Biochem. Sci.* **1996**, *21*, 460. (c) Goldbeter, A.; Koshland, D. E. *Proc. Natl. Acad. Sci. U. S. A.* **1981**, *78*, 6840.

(9) Carpenter, C. C.; Fischl, M. A.; Hammer, S. M.; Hirsch, M. S.; Jacobsen, D. M.; Katzenstein, D. A.; Montaner, J. S.; Richman, D. D.; Saag, M. S.; Schooley, R. T.; Thompson, M. A.; Vella, S.; Yeni, P. G.; Volberding, P. A. *JAMA* **1997**, *277*, 1962.

(10) Bullen, R. A.; Arnot, T. C.; Lakeman, J. B.; Walsh, F. C. *Biosens. Bioelectron.* **2006**, *21*, 2015.

(11) Privman, V.; Pedrosa, V.; Melnikov, D.; Pita, M.; Simonian, A.; Katz, E. *Biosens. Bioelectron.* **2009**, *25*, 695.

(12) Goodman, L. S.; Gilman, A.; Hardman, J. G.; Gilman, A. G.; Limbird, L. E. *Goodman & Gilman's The Pharmacological Basis of Therapeutics*, 9th ed.; McGraw-Hill Health Professions Division: New York, 1996.

(13) Vallée-Bélisle, A.; Ricci, F.; Plaxco, K. W. *J. Am. Chem. Soc.* **2012**, *134*, 2876.

(14) Kang, D.; Vallée-Bélisle, A.; Porchetta, A.; Plaxco, K. W.; Ricci, F. *Angew. Chem., Int. Ed.* **2012**, *51*, 6717.

(15) (a) Ricci, F.; Vallée-Bélisle, A.; Porchetta, A.; Plaxco, K. W. *J. Am. Chem. Soc.* **2012**, *134*, 15177. (b) Idili, A.; Plaxco, K. W.; Vallée-Bélisle, A.; Ricci, F. *ACS Nano* **2013**, *7*, 10863.

(16) (a) Porchetta, A.; Vallée-Bélisle, A.; Plaxco, K. W.; Ricci, F. *J. Am. Chem. Soc.* **2012**, *134*, 20601. (b) Simon, A. J.; Vallée-Bélisle, A.; Ricci, F.; Plaxco, K. W. *Proc. Natl. Acad. Sci. U. S. A.* **2014**, *111*, 15048. (c) Cheng, L.; Qu, H.; Teng, J.; Yao, L.; Xue, F.; Chen, W. *Food Sci. Hum. Wellness* **2017**, *6*, 70.

(17) Porchetta, A.; Vallée-Bélisle, A.; Plaxco, K. W.; Ricci, F. *J. Am. Chem. Soc.* **2013**, *135*, 13238.

(18) Idili, A.; Vallée-Bélisle, A.; Ricci, F. *J. Am. Chem. Soc.* **2014**, *136*, 5836.

(19) Gareau, D.; Desrosiers, A.; Vallée-Bélisle, A. *Nano Lett.* **2016**, *16*, 3976.

(20) (a) Le, V. S.; Jeong, J.-E.; Kim, B.; Lee, J.; Kyhm, K.; Woo, H. Y. *Sens. Actuators, B* **2017**, *240*, 810. (b) Zhang, H.; Jia, S.; Lv, M.; Shi, J.; Zuo, X.; Su, S.; Wang, L.; Huang, W.; Fan, C.; Huang, Q. *Anal. Chem.* **2014**, *86*, 4047.

(21) (a) Song, S.; Wang, L.; Li, J.; Fan, C.; Zhao, J. *TrAC, Trends Anal. Chem.* **2008**, *27*, 108. (b) Wu, L.; Zhang, X.; Liu, W.; Xiong, E.; Chen, J. *Anal. Chem.* **2013**, *85*, 8397. (c) Ren, K.; Wu, J.; Yan, F.; Ju, H. *Sci. Rep.* **2015**, *4*, 4360. (d) Cho, E. J.; Lee, J.; Ellington, A. D. *Annu. Rev. Anal. Chem.* **2009**, *2*, 241. (e) Liu, J.; Cao, Z.; Lu, Y. *Chem. Rev.* **2009**, *109*, 1948.

(22) (a) Luo, X. M.; McKeague, M.; Pitre, S.; Dumontier, M.; Green, J.; Golshani, A.; Derosa, M. C.; Dehne, F. *RNA* **2010**, *16*, 2252. (b) Zuo, X.; Song, S.; Zhang, J.; Pan, D.; Wang, L.; Fan, C. *J. Am. Chem. Soc.* **2007**, *129*, 1042. (c) Hasanzadeh, M.; Shadjou, N.; de la Guardia, M. *TrAC, Trends Anal. Chem.* **2017**, *89*, 119. (d) Wu, F.; Xiao, F.; Wu, Z.; Yu, R. *Anal. Chem.* **2017**, *89*, 2852. (e) Wei, B.; Zhang, J.; Wang, H.; Xia, F. *Analyst* **2016**, *141*, 4313.

(23) Labib, M.; Sargent, E. H.; Kelley, S. O. *Chem. Rev.* **2016**, *116*, 9001.

(24) Lubin, A. A.; Plaxco, K. W. *Acc. Chem. Res.* **2010**, *43*, 496.

(25) Nutiu, R.; Li, Y. *J. Am. Chem. Soc.* **2003**, *125*, 4771.

(26) Nutiu, R.; Li, Y. *Angew. Chem.* **2005**, *117*, 1085.

(27) Munzar, J. D.; Ng, A.; Corrado, M.; Juncker, D. *Chem. Sci.* **2017**, *8*, 2251.

(28) Fan, C.; Plaxco, K. W.; Heeger, A. J. *Proc. Natl. Acad. Sci. U. S. A.* **2003**, *100*, 9134.

(29) Walter, A.; Wu, J.; Flechsig, G.; Haake, D. A.; Wang, J. *Anal. Chim. Acta* **2011**, *689*, 29.

(30) Yang, W.; Lai, R. Y. *Electrochem. Commun.* **2011**, *13*, 989.

(31) Xiang, Y.; Qian, X.; Chen, Y.; Zhang, Y.; Chai, Y.; Yuan, R. *Chem. Commun.* **2011**, *47*, 2080.

(32) Vallée-Bélisle, A.; Ricci, F.; Plaxco, K. W. *Proc. Natl. Acad. Sci. U. S. A.* **2009**, *106*, 13802.

(33) Buchler, N. E.; Cross, F. R. *Mol. Syst. Biol.* **2009**, *5*, 272.

(34) Buchler, N. E.; Louis, M. *J. Mol. Biol.* **2008**, *384*, 1106.

(35) Ricci, F.; Vallee-Belisle, A.; Plaxco, K. W. *PLoS Comput. Biol.* **2011**, *7*, e1002171.

(36) Beis, I.; Newsholme, E. A. *Biochem. J.* **1975**, *152*, 23.

(37) White, R. J.; Phares, N.; Lubin, A.; Xiao, Y.; Plaxco, K. W. *Langmuir* **2008**, *24*, 10513.

(38) McKeating, K. S.; Aubé, A.; Masson, J. *Analyst* **2016**, *141*, 429.

(39) (a) Stojanovic, M. N.; Stefanovic, D. *Nat. Biotechnol.* **2003**, *21*, 1069. (b) Kang, D.; White, R. J.; Xia, F.; Zuo, X.; Vallée-Bélisle, A.; Plaxco, K. W. *NPG Asia Mater.* **2012**, *4*, e1.